Consideration of Magnetic Flux Distribution in Multi−Filamented $YBa_2Cu_3O_{7-\delta}$ films by controlling crystal array using surface−modified substrate

Hiroki Fujimoto, Akiyoshi Matsumoto, Shuuichi Ooi, Minoru Tachiki, Ryo Teranishi

***Abstract*—Large direct currents can flow through $REBa_2Cu_3O_{7-\delta}$ (REBCO) wires without energy loss because of zero resistance. However, they suffer from alternating current (AC) loss. Here, a multifilament is produced by creating areas with disordered $YBa_2Cu_3O_{7-\delta}$ (YBCO) using the metal−organic deposition method on $SrTiO_3$ substrates with Zr patterning. YBCO crystal orientation without Zr patterning was ordered, whereas it was disordered in the sample with Zr patterning. Additionally, controlling the YBCO crystal array correlated with superconductivity and enabled it to be a multifilament. Therefore, this method can realize AC loss reduction.**

***Index Terms*—Coated conductors, Multi−filamentary superconductors, YBCO, magnetic flux distribution.**

I. INTRODUCTION

REBa$_2$Cu$_3$O$_{7-\delta}$ (REBCO) has a triple perovskite structure and is characterized by a high critical temperature (T_c) and critical current density (J_c) [1]. When focusing on J_c, the a, b, and c axes of crystals must be aligned as closely as possible using a substrate with crystal lattice constants similar to those of REBCO crystals [2]. This is because high current can be obtained by aligning CuO_2 planes. Thus, REBCO is applied as thin film wires called the “coated conductor (CC)” [3]. REBCO CCs have been optimized in recent years; both direct current (DC) and alternating current (AC) have been used in REBCO CCs [4−12]. REBCO CCs can be used in power transmission line cables and magnetic coils [13−18]. However, REBCO CCs show large AC loss [19−24]. REBCO CCs are a type II superconductor, implying that they are in a mixed state and allow the magnetic flux to penetrate the superconductor. In AC, the internal magnetic field changes with current. Because of this change, the Lorentz force on the magnetic flux increases owing to electromagnetic induction. Therefore, the magnetic flux begins to move, which generates work and energy loss. This energy loss leads to AC loss.

Submitted for review September 26, 2023. This work was supported by JSPS KAKENHI grant numbers 21K18831 and 22H0219. This study was partially supported by the Joint Research Hub Program of the National Institute for Materials Science, Japan.

Hiroki Fujimoto is with Department of Materials, Kyushu University, 744 Motooka, Nishi−ku, Fukuoka 819−0395, Japan (e−mail: fujimoto.hiroki.779@s.kyushu−u.ac.jp).

Akiyoshi Matsumoto is with the National Institute for Materials Science, Tsukuba, Ibaraki 3050047, Japan (e−mail: matsumoto.akiyoshi@nims.go.jp).

Shuuichi Ooi is with the National Institute for Materials Science, Tsukuba, Ibaraki 3050047, Japan (e−mail: ooi.shuuichi@nims.go.jp).

Minoru Tachiki is with the National Institute for Materials Science, Tsukuba, Ibaraki 3050047, Japan (e−mail: tachiki.minoru@nims.go.jp).

Ryo Teranishi is with Department of Materials, Kyushu University, 744 Motooka, Nishi−ku, Fukuoka 819−0395, Japan (e−mail: teranishi@zaiko.kyushu−u.ac.jp).

To reduce AC loss, the superconducting layer of the CC is divided into multiple filaments. Several studies have been recently conducted on dividing into multiple filaments [25−32], which has been achieved using two major methods. In the first method, a multifilament is produced by laser scribing (post−processing) [25−27], which has been confirmed to reduce AC loss by a factor of five by dividing the REBCO layer into five sections in the width direction [28]. However, dross produced by laser scribing remains between the filaments, causing incomplete insulations. Although the dross can be reduced by an over-etching, this process induces a decrease of J_c and cannot eliminate the dross perfectly [27], [33]. In addition, the equipment is not inexpensive, and the process is complex.

In the second method, a multifilament is produced by patterning the insulator via the ink−jet method on a buffer layer, followed by superconducting layer deposition (pre−processing) [32]. This method has been confirmed to reduce AC loss by a factor of 10. Because the insulator width is ~ 200 μm, the number of filaments that can be made on the substrate in this manner is limited.

Herein, we report another method by intentionally patterning a material with crystal lattice constants not similar to those of YBCO crystals, on the substrate and depositing a film. The YBCO layer is divided in two parts: ordered and disordered [34]. We focus on the evaluation of superconducting property using a magneto-optical (MO) imaging technique. The MO image shows the flux penetrated in the bright parts but not in the dark ones [35], [36]. A previous study investigated the crystal orientation of an electron backscatter diffraction (EBSD) image and showed that the YBCO crystals on the substrate were ordered in the white parts, while those on Zr were disordered in the black parts [34]. This indicates that MO observation is an advantageous method to determine whether YBCO is divided into multi−filaments. Moreover, MO observation is helpful to understand the difference between the parts which the flux penetrates or not.

In this study, we aim to consider the magnetic flux distribution in multi−filament YBCO films by controlling crystal array using a surface−modified substrate.

II. Experimental Method

Owing to the dependency of the YBCO orientation on lattice consistency, Zr was used as a lattice mismatch material for YBCO in this study. $SrTiO_3$ (STO) with an orientation of (100) and dimension of 5.0 mm × 5.0 mm × 1.0 mm was used as substrate with Zr patterning. Also, STO substrate with dimension of 10 mm × 10 mm × 1.0 mm was used as the one, without Zr patterning. The substrate with Zr patterning had a width of 5−20 µm as shown in Fig. 1(a). Patterning was performed via photolithography [37]; its procedure is as follows (Fig. 1(b)).

First, a resist was deposited on the substrate, and a laser beam was applied to pattern the areas where the impurities were to be deposited. Subsequently, the resist was removed from the patterned area and Zr was sputtered. Finally, the remaining resist was removed to complete Zr patterning. Before film formation, the height and width of Zr on the prepared substrate were evaluated using a laser microscope.

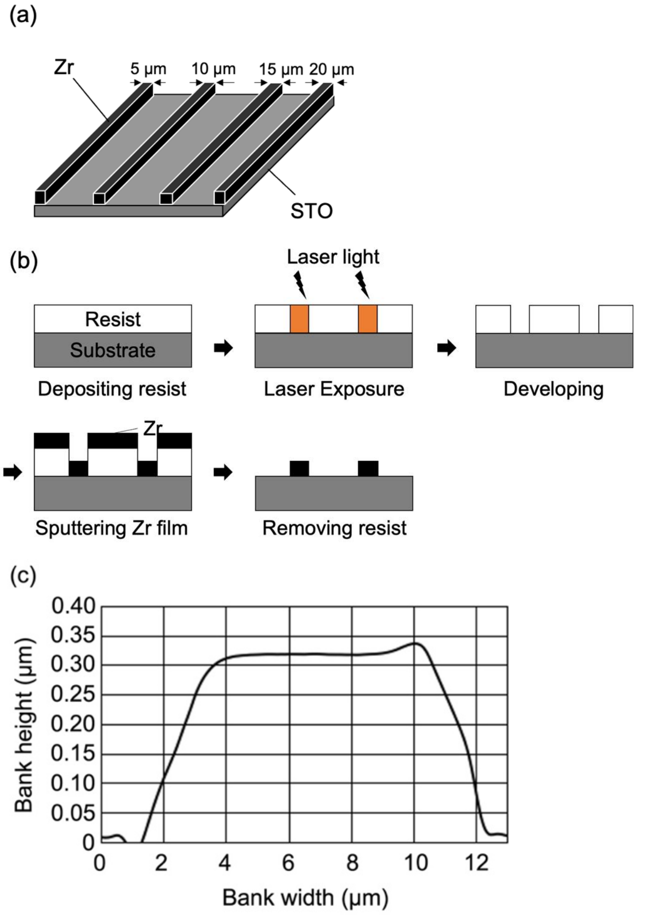

Fig. 1. View of Zr patterning on substrates. (a) Diagram of Zr patterning. (b) Photolithography procedure. (c) Laser microscopy observations of the Zr bank.

The samples were prepared using a metal−organic deposition (MOD) method. Y, Ba, and Cu were dissolved into an octanone solution with a molar ratio of Y:Ba:Cu = 1:1.5:3. The film formation method using the solution is as follows: the solution was spin coated on the substrates at 3,000 rpm for 2 min, and the samples were calcinated at 703 K. These steps were repeated thrice to obtain a YBCO film thickness of ~ 0.6 µm. The calcined samples were then crystallized at 1,053 K and annealed in an oxygen atmosphere.

After film formation, the samples were subjected to X−ray diffraction (XRD) to identify the crystal formation, scanning electron microscopy (SEM) for surface observation, the four−terminal method for T_c evaluation, and MO measurement for magnetic flux distribution [35].

III. Results and Discussion

Laser microscopy was employed to examine the substrate with a 10 µm wide Zr stripe, as shown in Fig. 1(c). The height of the bank was ~ 0.32 µm. The upper sole was ~ 60% longer than the lower sole. The base angles of the left and right sides were 81.7° and 81.1°, respectively. This shows that the Zr stripe was approximately an isosceles trapezoid.

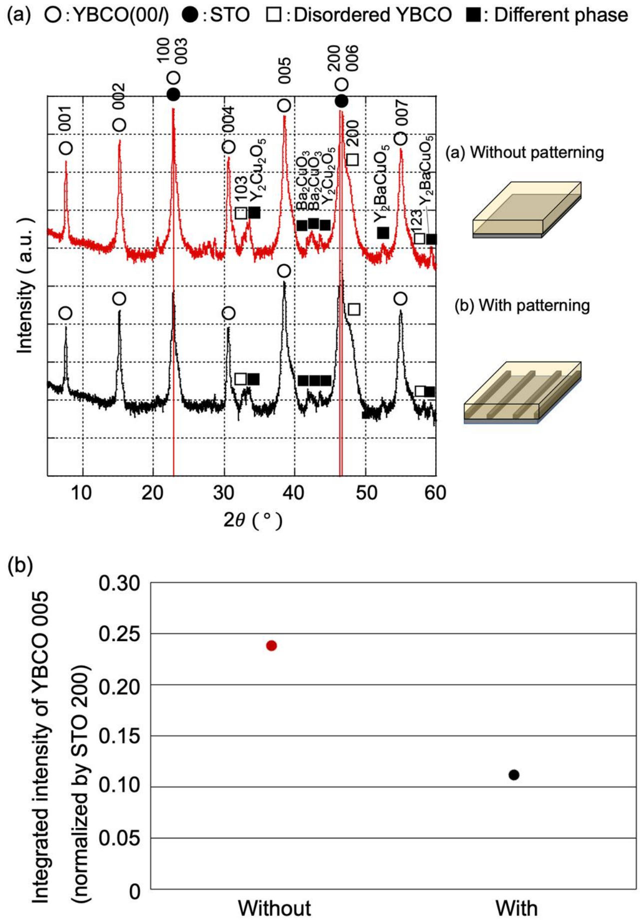

Fig. 2. XRD patterns of the fabricated YBCO film with and without Zr patterning. (a) Results of Cu−Kα θ−2θ scan. (b) Integrated strength of YBCO 005 normalized by STO 200.

Fig. 2 shows the XRD patterns of the fabricated YBCO film with and without Zr patterning. Fig. 2(a) shows the results of θ−2θ scan. In addition to other peaks, the 00*l* peaks of YBCO were observed in the film without Zr patterning. Among these, the largest peak at 33.2° corresponded to the 103 plane of YBCO. The peak intensity was approximately a quarter of the 004 peak of YBCO. For the film with Zr patterning, the 00*l* and disordered YBCO peaks were also observed. The peak intensity of disordered YBCO with Zr patterning was similar to that without Zr patterning.

To measure the change in the YBCO 00*l* peak intensity with and without patterning, the integrated intensity of the YBCO 005 peak normalized by the STO 200 peak was considered. (Fig. 2(b)). The integral strength of the YBCO 005 peak without and with Zr patterning was 0.24 and 0.11, respectively. This shows that the volume of ordered YBCO crystals with Zr patterning was 46.9% less than that without Zr patterning, indicating that the volume of the oriented YBCO crystals decreased upon Zr patterning.

Furthermore, the crystals were found to be uniformly spread in Fig. 3(a), whereas in Fig. 3(b) a dark area, representing sample surface irregularities, is observed at the center of the left image at a width of ~ 12.2 μm from edge to edge in the vertical direction. The dark area was also observed from the edge to edge of the substrate. This is believed to be due to Zr patterning. At high magnification, it was confirmed that crystals were densely present in both (a) and (b). The disordered crystal structure extended in the vertical direction on the right side of the image in (b). The border between the dense and disordered crystals was not clear. The other parts of (b) were the same as those in (a). In addition, the sizes of white solids were 0.35−0.60 μm in (a) and 0.45−0.70 μm in (b). Additionally, the number of white solids in (b) was more than that in (a).

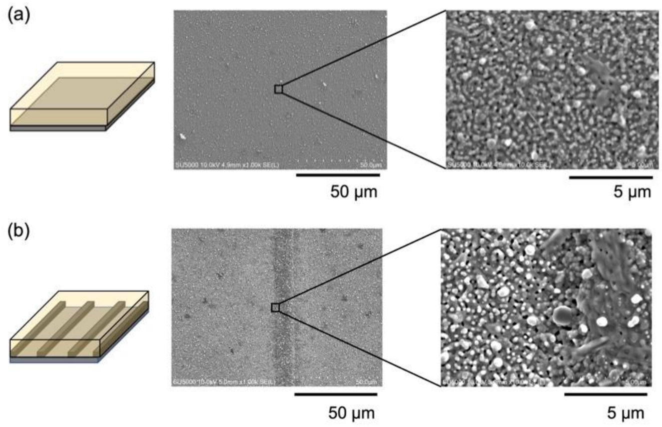

Fig. 3. SEM images of the sample surface (a) without and (b) with Zr patterning.

Based on these observations, the following inferences could be drawn. The contrast in (b) was due to Zr patterning. Zr patterning also contributed to the disorder of the crystal structure in (b). This contribution to crystal disorder was considered on not only the top surface of the Zr bank but also its side. Moreover, the white solids were precipitates derived from Y and Cu [38]. This is because the sample fabricated using a raw material solution containing of Y, Ba, and Cu shifted to a 1:1.5:3 ratio. The volume reduction of the YBCO 00*l* crystals corresponded to the disorder of the crystal structure according to the results shown in Fig. 2(b).

Moreover, T_c^{onset} and T_c^{zero} of the sample without Zr patterning measured by the four−terminal method were 86.6 K and 86.0 K, respectively. The difference in temperature (ΔT) between the two points at 90% and 10% of the extrapolated value from the normal conduction transition was 0.4 K.

Fig. 4 shows the magnetic flux distribution of the sample with Zr patterning at 5 K and 200 Oe. This image was recorded from a top view with the magnetic flux applied perpendicular to the surface. The bright and dark regions in the sample with Zr patterning corresponded to the regions which the magnetic flux penetrated and did not penetrate, respectively.

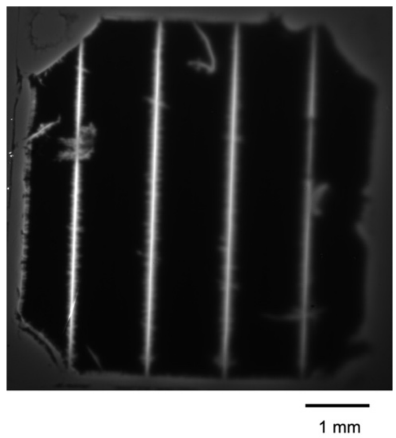

Fig. 4. MO image of the sample with Zr patterning at 5 K and 200 Oe.

Four straight vertical bright lines is clearly observed at equal intervals. Also, uniform dark areas were observed between the lines. The width of the bright lines was 90−160 μm. These results indicates that the bright lines were formed because the substrate had four banks of Zr. The bright areas corresponded to the areas where the magnetic flux penetrated. The superconductivity of the four bright lines was found to be broken or low. Comparing with the magnetic flux distribution with the SEM image of Fig. 3(b), it is recognized that the bright lines and dark areas of the MO image are corresponding to the disordered crystal region and the ordered crystal regions of the YBCO film, respectively. The dark areas exhibited the Meissner effect and/or shielding effect owing to the good orientation of YBCO. Thus, the magnetic distribution correlated with the microstructure images. This correlation suggested that the boundary between bright and dark regions in Fig. 4 because ordered and disordered crystals were mixed at the edge of Zr patterning in Fig. 3(b).

According to the results shown in Figs. 2, 3, and 4, the samples without Zr patterning consisted of ordered YBCO (Fig. 5(a)), whereas ones with Zr patterning consisted of disordered YBCO on Zr (Fig. 5(b)). That is Zr patterning enabled the formation of multiple filaments of YBCO.

The field distribution views of Fig. 5 (b) along the b−axis are shown in (c), respectively. ~~The views of Figs. 5 (a) and (b) along the a−axis are shown in (c) and (d), respectively.~~ The intergranular current mainly flowed in ordered YBCO, and the shielding current flowing through the crystal was large. ~~The magnetic flux was therefore uniformly shielded.~~ In contrast, only intragranular current mainly flowed in disordered YBCO, the shielding current flowing through the crystal was small~~, and that the magnetic flux was not shielded~~. Therefore, magnetic flux penetrates the disordered YBCO shielded by the oriented YBCO. Comparing this with Fig. 4 results, the black areas uniformly shielded the magnetic flux as opposed to the white areas. This suggested that the YBCO crystal array correlated with the magnetic flux distribution.

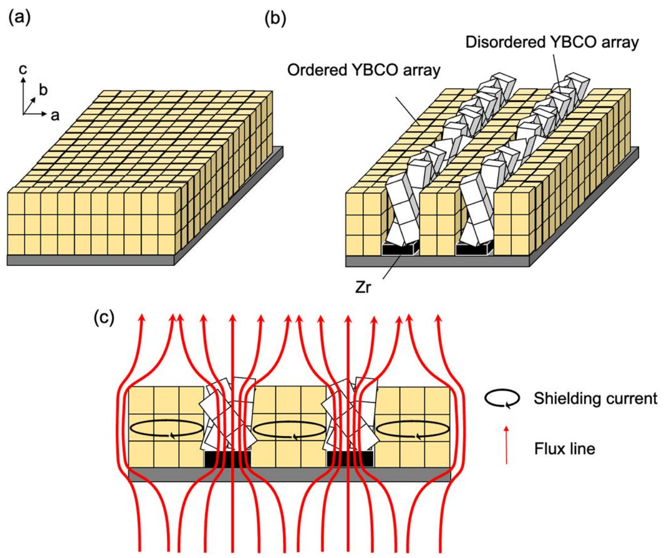

Fig. 5. Schematic of YBCO crystal orientation (a) without and (b) with patterning, and the difference in magnetic flux behavior for (c) ordered YBCO and (d) disordered YBCO.

IV. Conclusion

Herein, we discussed the differences in superconducting properties exhibited by different orientations of YBCO films fabricated on substrates patterned with a lattice mismatch material to YBCO.

We selected Zr as a lattice mismatch material to YBCO and prepared 5–20 μm−wide stripes on the substrate. YBCO films were fabricated on substrates with and without Zr patterning via MOD process. The sample without Zr patterning consisted of ordered YBCO crystals. In contrast, the sample with Zr patterning had parts of the bank with disordered YBCO crystals and parts with ordered YBCO crystals. Therefore, Zr patterning allowed the control of the YBCO crystal array through simple heat treatment without any post−processing. Magnetic evaluation confirmed that a division existed between the areas where superconductivity was observed and broken. These results indicated that the crystal array pattern matched that of the magnetic flux passing through. Therefore, the crystal array control correlated with magnetic flux distribution, and Zr patterning led to the formation of the YBCO multifilament. Thus, this method serves as a novel approach to reduce AC loss.

References

[1] J. A. Smith, M. J. Cima, and N. Sonnenberg, "High Critical Current Density Thick MOD-Derived YBCO Films," *IEEE Trans. Appl. Supercond*., vol. 9, No. 2, pp. 1531−1534, Jun. 1999.

[2] D. Dimos, P. Chaudhari, J. Mnnhart, and F. K. Legoues, Orientation "Dependence of Grain-Boundary Critical Currents in $YBa_2Cu_3O_{7-\delta}$ Bicrystals," *Phys. Rev. Lett*., vol. 61, 1988, Art. No. 219.

[3] M. P. Paranthaman, and T. Izumi, Guest Editors, "High-Performance YBCO-Coated Superconductor Wires" *MRS BULLETIN*, vol. 29, No. 8, pp. 533−541, 2004.

[4] C. Senatore, C. Barth, M. Bonura, M. Kulich, and G. Mondonico, "Field and temperature scaling of the critical current density in commercial REBCO coated conductors" *Supercond. Sci. Technol*., vol. 29, 2015, Art No. 014002.

[5] Y. Iijima, N. Tanabe, O. Kohno, Y. Ikeno, "In-plane aligned $YBa_2Cu_3O_{7-x}$ thin films deposited on polycrystalline metallic substrates," *Appl. Phys. Lett*., vol. 60, pp. 769−771, 1992.

[6] A. Goyal, D. P. Norton, J. D. Budai, M. Paranthaman, E. D. Specht, D. M. Kroeger, D. K. Christen, Q. He, B. Saffian, F. A. List, D. F. Lee, P. M. Martin, C. E. Klabunde, E. Hartfield, V. K. Sikka, "High critical current density superconducting tapes by epitaxial deposition of YBa_2Cu_3Ox thick films on biaxially textured metals," *Appl. Phys. Lett*., vol. 69, pp. 1795−1797, 1996.

[7] D. Uglietti, "A review of commercial high temperature superconducting materials for large magnets: from wires and tapes to cables and conductors," *Supercond. Sci. Technol*., vol. 32, 2019, Art No. 053001.

[8] A. Usokin, U. Betz, J. Gnilsen, S. Noll-Baumann, and K. Schlenga, "Long-length YBCO coated conductors for ultra-high field applications: gaining engineering current density via pulsed laser deposition/alternating beam-assisted deposition route," *Supercond. Sci. Technol*., vol. 32, 2019, Art No. 053001.

[9] W. Prusseit, M. Bauer, V. Groβe, R. Semerad, G. Sigl, M. Dürrschnabel, Z. Aabdin, O. Eibl, "Working around HTS Thickness Limitations – towards 1000+ A/cm – Class Coated Conductors," *Physics Procedia*, vol. 36, pp. 1417−1422, 2012.

[10] A. Sundaram, Y. Zhang, A. R. Knoll, D. Abraimov, P. Brownsey, M. Kasahara, G. M. Carota, R. Nakasaki, J. B. Cameron, G. Schwab, L. V. Hope, R. M. Schmidt, H. Kuraseko, T. Fukushima, and D. W. Hazelton, "2G HTS wires made on 30 μm thick Hastelloy substrate," *Supercond. Sci. Technol*., vol. 29, 2016, Art No. 104007.

[11] J. -H. Lee, H. Lee, J. -W. Lee, S. -M. Choi, S. -I. Yoo, and S. -H. Moon, "RCE-DR, a novel process for coated conductor fabrication with high performance," *Supercond. Sci. Technol*., vol. 27, 2014, Art No. 044018.

[12] Y. Zhao, J-M. Zhu, G-Y. Jiang, C-S. Chen, W. Wu, Z-W. Zhang, S. K. Chen, Y. M. Hong, Z-J. Jin, and Y. Yamada, "Progress in fabrication of second generation high temperature superconducting tape at Shanghai Superconductor Technology," *Supercond. Sci. Technol*., vol. 32, 2019, Art No. 044004.

[13] M. Yagi, S. Mukoyama, N. Amemiya, A. Ishiyama, X. Wang, Y. Aoki, T. Saito, T. Ohkuma, and O. Maruyama, "Progress of 275 kV–3 kA YBCO HTS cable," *Physica C*, vol. 471, pp. 1274−1278, 2011.

[14] O. Maruyama, T. Ohkuma, T. Masuda, Y. Ashibe, S. Mukoyama, M. Yagi, T. Saitoh, T. Hasegawa, N. Amemiya, A. Ishiyama, and N. Hayakawa, "Development of 66 kV and 275 kV Class REBCO HTS Power Cables," *IEEE Trans. Appl. Supercond*., vol. 23, no. 3, Jun. 2013, Art. no. 5401405.

[15] M. Iwakuma, H. Hayashi, H. Okamoto, A. Tomioka, T. Saito, Y. Iijima, Y. Suzuki, S. Yoshida, Y. Yamada, and Y. Shiohara, "Development of REBCO superconducting power transformers in Japan," *Physica C*, vol. 469, pp. 1726−1732, 2009.

[16] W. D. Markiewicz, D. C. Larbalestier, H. W. Weijers, A. J. Voran, A. J. Voran, K. W. Pickard, W. R. Sheppard, J. Jaroszynski, A. Xu, R. P. Walsh, J. Lu, A. V. Gavrilin, and P. D. Noyes, "Design of a Superconducting 32 T Magnet With REBCO High Field Coils," *IEEE Trans. Appl. Supercond*., vol. 22, no. 3, Jun. 2012, Art. no. 4300704.

[17] J. Bascuñán, S. Hahn, D. K. Park, Y. Kim, and Y. Iwasa, "On the 600MHz HTS Insert for a 1.3 GHz NMR Magnet," *IEEE Trans. Appl.*

Supercond., vol. 22, no. 3, Jun. 2012, Art. no. 4302104.

[18] L. Rossi, A. Badel, M. Bajko, A. Ballarino, L. Bottura, M. M. J. Dhallé, M. Durante, Ph. Fazilleau, J. Fleiter, W. Goldacker, E. Härö, A. Kario, G. Kirby, C. Lorin, J. van Nugteren, G. de Rijk, T. Salmi, C. Senatore, A. Stenvall, P. Tixador, A. Usoskin, G. Volpini, Y. Yang, and N. Zangenberg, "The EuCARD-2 Future Magnets European Collaboration for Accelerator-Quality HTS Magnets," *IEEE Trans. Appl. Supercond*., vol. 25, no. 3, Jun. 2015, Art. no. 4001007.

[19] E. H. Brandt and M. Indenbom, "Type-II-superconductor strip with current in a perpendicular magnetic field" *Phys. Rev. B*, vol. 48, no. 17, May. 1993, Art. no. 12893.

[20] N. Amemiya, S. Murasawa, N. Banno, and K. Miyamoto, "Numerical modelings of superconducting wires for AC loss calculations," *Physica C*, vol. 310, pp. 16−29, 1998.

[21] N. Amemiya, K. Yoda, S. Kasai, Z. Jiang, G. A. Levin, P. N. Barnes, and C. E.Oberly, "AC Loss Characteristics of Multifilamentary YBCO Coated Conductors" *IEEE Trans. Appl. Supercond*., vol. 15, no. 2, pp. 1637−1642, 2005.

[22] T. Nishioka, N. Amemiya, N. Enomoto, Z. Jiang, Y. Yamada, T. Izumi, Y. Siohara, T. Saitoh, Y. Iijima, and K. Kakimoto, "AC Loss of YBCO Coated Conductors Fabricated by IBAD/PLD Method," *IEEE Trans. Appl. Supercond*., vol. 15, no.2, 2843−2846 (2005).

[23] M. D. Ainslie, C. W. Bumby, Z. Jiang, R. Toyomoto, and N. Amemiya, "Numerical modelling of dynamic resistance in high-temperature superconducting coated-conductor wires," *Supercond. Sci. Technol*., vol. 31, 2018, Art. no. 074003.

[24] Y. Sogabe, Z. Jiang, S. C. Wimbush, N. M. Strickland, M. Staines, N. J. Long, and N. Amemiya, "AC Loss Characteristics in REBCO Coil Assemblies With Different Geometries and Conductors," *IEEE Trans. Appl. Supercond*., vol. 28, no. 3, 4700105 (2018).

[25] S. Terzieva, M. Vojenciak, F. Grilli, R. Nast, J. Šouc, W. Goldacker, A. Jung, A. Kudymow, and A. Kling, "Investigation of the effect of striated strands on the AC losses of 2G Roebel cables," *Supercond. Sci. Technol*., vol. 24, 2011, Art. no. 045001.

[26] M. D. Sumption, E. W. Collings, and P. N. Barnes, "AC Loss in Striped (Filamentary) YBCO Coated Conductors Leading to Designs for High Frequencies and Field-Sweep Amplitudes," *Supercond. Sci. Technol*., vol. 18, 2005, Art. no. 122.

[27] T. Machi, K. Nakao, T. Kato, T. Hirayama, and K. Tanabe, "Reliable fabrication process for long-length multi-filamentary coated conductors by a laser scribing method for reduction of AC loss," *Supercond. Sci. Technol*., vol. 26, 2013, Art. no. 105016.

[28] Y. Shiohara, T. Taneda, and M. Yoshizumi, "Overview of Materials and Power Applications of Coated Conductors Project," *Jpn. J. Appl. Phys*., vol. 51, 2012, Art. no. 017007.

[29] A. C. Wulff, M. Solovyov, F. Gömöry, A. B. Abrahamsen, O. V. Mishin, A. Usoskin, A. Rutt, J. H. Lundeman, K. Thydén, J. B. Hansen, and J-C Grivel, "Two level undercut-profile substrate for filamentary $YBa_2Cu_3O_7$ coated conductors," *Supercond. Sci. Technol*., vol, 28, 2015, Art. no. 072001.

[30] S. Fujita, S. Muto, C. Kurihara, H. Sato, W. Hirata, N. Nakamura, M. Igarashi, S. Hanyu, M. Daibo, Y. Iijima, K. Naoe, M. Iwakuma, and T. Kiss, "Characterization of Multifilamentary REBCO Coated Conductor Coil Fabricated by Using the Process of Scratching the IBAD-MgO Layer," *IEEE Trans. Appl. Supercond*., vol. 27, no. 4, 2017, Art. no. 6600504.

[31] X. Jin, H. Oguro, Y. Oshima, T. Matsuda, and H. Maeda, "Development of a $REBa_2Cu_3O_{7-\delta}$ multi-core superconductor with 'inner split' technology," *Supercond. Sci. Technol*., vol. 29, 2016, Art. no. 045006.

[32] X. Cai, I. Kesgin, R. Schmidt, Y. Chen, and V. Selvamanickam, "Completely Etch-Free Fabrication of Multifilamentary Coated Conductor Using Inkjet Printing and Electrodeposition," *IEEE Trans. Appl. Supercond*., vol. 23, no. 3, Jun. 2013, Art. no. 6603005.

[33] K. Katayama, T. Machi, T. Nakamura, Y. Takagi, K. Nakaoka, M.Yoshizumi, T. Izumi, and Y. Shiohara, "Development of low AC loss TFA−MOD coated conductors," *Physics Procedia*, vol. 58, pp. 142−145, 2014.

[34] A. Matsumoto, M. Tachiki, and S. Ooi, "Development of YBCO Patterned Multi-Filamentary Film Using Photolithography Method," *IEEE Trans. Appl. Supercond*., vol. 33, no. 5, Aug. 2013, Art. no. 7500404.

[35] S. Ooi, M. Tachiki, T. Konomi, T. Kubo, A. Kikuchi, S. Arisawa, H. Ito, and K. Umemori, "Observation of intermediate mixed state in high-purity cavity-grade Nb by magneto-optical imaging," *Phys. Rev. B*, vol. 104, 2021, Art. no. 064504.

[36] Th. Schuster, M. R. Koblischka, H. Kuhn, H. Kronmüller, G. Friedl, B. Roas, L. Schultz, "Flux penetration into $YBa_2Cu_3O_x$ thin films covering substrate step edges," *Appl. Phys. Lett.*, vol. 62, pp. 768−770, 1993.

[37] D. Panjwani, M. Yesiltas, J. Nath, D. E. Maukonen, I. Rezadad, E. M. Smith, R. E. Peale, C. Hirschmugl, J. Sedlmair, R. Wehlitz, M. Unger, and G. Boreman, "Patterning of oxide-hardened gold black by photolithography and metal lift-off," *Infrared Phys. Technol*., vol. 62, pp. 94−99, 2014.

[38] R. Teranishi, K. Tada, J. Yoshida, K. Yamada, N. Mori, M. Mukaida, M. Inoue, T. Kiss, K. Nakaoka, M. Miura, M. Yoshizumi, T. Izumi, and Y. Shiohara, "High-Jc YBCO films using precursors with barium concentration gradient in film thickness by TFA-MOD process," *Physica C*, vol. 469, pp. 1345–1348, 2009.